

Supplemental Materials

Molecular Biology of the Cell

Ivanovska et al.

Cross-linked matrix rigidity and soluble retinoids synergize in nuclear lamina regulation of stem cell differentiation

Irena L. Ivanovska et al.

Supplemental materials

Supplemental materials and methods

Supplemental figures S1 – S7

Supplemental references

Supplemental materials and methods

Cell Culture Human-derived alveolar epithelial (A549, CCL-185) cells were cultured according to protocols provided by the supplier (American Type Culture Collection). Primary human mesenchymal stem cells (anonymous donors with Institutional Review Board approvals) were obtained from the Xenograft Core Facility at the University of Pennsylvania School of Medicine. They were cultured in low glucose Dulbecco's modification of Eagle's medium (DMEM, Invitrogen) with 10% fetal bovine serum (FBS, Sigma Aldrich).

Mesenchymal differentiation of iPSCs without EB formation. iPSC lines were derived from primary fibroblasts and were obtained from 'The Progeria Research Foundation Cell & Tissue Bank', Univ. Ottawa. Derivation of iPSC-MSCs is done as described in (Zou *et al.*, 2013), briefly three days after splitting, iPS medium was replaced with MSC medium, which consisted of low glucose Dulbecco's modification of Eagle's medium (DMEM, Invitrogen) with 10% fetal bovine serum (FBS, Sigma Aldrich) and 1% penicillin/streptomycin. The MSC medium was changed every 2 days. After 14 days culture, the cells were trypsinized (0.25% trypsin/1 mM EDTA, Difco-Sigma) and expanded in MSC medium on 0.1% gelatin coated dishes (Becton Dickinson). When confluent (3–5 days), cells were harvested with 0.025% trypsin-EDTA and then regularly passaged at a 1:3 ratio. Usually, after the third trypsinization, a morphologically homogeneous population of fibroblast-like cells became evident and was used in the analysis of MSC phenotypic characteristics and differentiation potential.

Lamin knockdown. Cells were passaged to 70% confluency 24 hr before transfection.

A complex of siRNA (30 nM; siLMNA1, 5'-GGUGGUGACGAUCUGGGCU-3' or siLMNA2, 5'- AACUGGACUCCAGAAGAACAUC-3') was transfected into cells with Lipofectamine 2000 reagent (1 µg/mL) as described in the manufacturer's protocol (Invitrogen).

Drug treatment protocol. Cultured cells were treated with control solvent (0.15% EtOH, 0.15% DMSO in media with 10% FBS), or solvent containing: all-trans RA (1 µM, Fisher Scientific); adapalene; CD437 (0.1 µM, Tocris Bioscience); CD1530; CD2665 (1 µM, Tocris Bioscience); AGN-193109 (1 µM, Santa Cruz Biotechnology).

Preparation of stiff substrates. Polyacrylamide hydrogels of 0.3 kPa to 40 kPa stiffness were prepared as described previously (Buxboim *et al.*, 2010). Gels for cell culture were further coated with type-I rat tail collagen or freshly prepared human fibronectin (BD Biosciences) as follows: Sulfo-Sanpah (Fisher Scientific) was dissolved in 50 mM, pH 8 HEPES to a concentration of 0.5 mg/mL and pipetted to form a complete coverage of the gels. Gels were placed inside a UV chamber and illuminated for 10 min by 365 nm illumination. To minimize collagen fiber formation, collagen was first mixed in equal volume of 4 °C 0.1 M acetic acid (Fisher Scientific) and then diluted in 4 °C 50 mM, pH 8 HEPES to a final concentration of 0.2 mg/mL. Protein was incubated on the gels while on a shaker overnight at 37 °C. Prior to seeding cells, gels were UV-sterilized in cell culture hood for two hours. Gels were kept hydrated in PBS or deionized water during all preparation steps.

Immunofluorescence imaging. Cells were rinsed with PBS, fixed with 4% paraformaldehyde (Fisher) for 20 min, washed twice with PBS and permeabilized with 0.5% Triton-X (Fisher) in PBS for 20 min. Cells were then treated with 5% BSA (blocking solution) for 1 hr. Following two additional PBS washes, samples were incubated overnight with primary antibodies at 1:300 dilution in 2% BSA solution with gentle agitation at 4 °C. The primary antibodies used were: lamin-A/C mouse monoclonal sc-7292; lamin-B goat polyclonal sc-6217; RAR-gamma rabbit polyclonal PA5-21463 (Thermo Scientific). Cells were washed twice in PBS and incubated with the corresponding secondary antibodies at 1:500 dilution for 45 minutes (Alexa Fluor 546, 594 and 647 nm; Invitrogen). Adherent cells on gels or glass coverslips were mounted with mounting media (Invitrogen ProLong Gold Antifade Reagent) or sometimes imaged with fixation and no mounting. Images of adherent cells were taken with an Olympus IX71 microscope in epifluorescence or else a confocal laser scanning mode with the 488 nm and 543 nm laser lines, for GFP and Alexa 546 dyes, respectively. All images for quantitative analysis in a given experiment were taken under the same imaging conditions.

mRNA profiling of tissues and cells. Human and mouse tissue transcript data (1.0 ST datasets) was downloaded from: http://www.affymetrix.com/support/technical/sample_data/exon_array_data.affx.

Transcriptomes from whole genome microarrays (Affymetrix, Santa Clara, CA) were for mouse adult tissues: brain, heart, kidney, liver, lung, ovary, muscle, spleen, testis and thymus ($n = 3$); and human adult tissues: brain, breast, heart, kidney, liver, pancreas, prostate, muscle, spleen, testis and thyroid ($n = 3$). Pearson correlations between *Col1a1* and a range of genes were calculated from these data sets using Mathematica (Wolfram) (Figs. 2 B, C).

mRNA levels were profiled in MSCs subjected to lamin-A,C knockdown ($n = 3$) (Fig. S6B). Total RNA was extracted from cells using Trizol and isolated by RNeasy (Qiagen) according to manufacturer's protocol. Total RNA was amplified and converted to cDNA using WT-Ovation Pico kit (NuGen) and converted to ST-cDNA, fragmented and biotin-functionalized using WT-Ovation Exon Module (NuGen). Hybridization cocktails were prepared at 45.4, 15.1 and 7.6 ng/ μ L ST-cDNA and mixed with Eukaryotic Hybridization Controls (GeneChip) at proportional concentrations. Each Sample was interrogated by sequential hybridization, rinse and scan cycles on a single Human Gene 1.0 ST DNA microarray (Affymetrix, Santa Clara, CA), from low to high concentration, and followed by two rinse-scan cycles in which no sample was added. In each experiment the scanned intensities that were obtained from all samples, five scans per array, were mutually RMA-summarized to transcription clusters gene levels so that the average and standard deviation could be calculated for each gene.

Quantitative mass spectrometry (MS). We have previously described methods for preparing primary tissue samples for MS (Swift *et al.*, 2013b) and for quantifying species-specific peptides (Swift *et al.*, 2013a). Briefly, tissue samples were flash-frozen in liquid nitrogen and finely ground between metal plates on dry ice. Proteins were then solubilized in 1x NuPAGE LDS buffer (with protease inhibitor cocktail and 0.1% β -mercaptoethanol) using sonication and heating (80 °C, 10 mins). Insoluble material was separated by centrifugation. SDS-PAGE gels (NuPAGE 4-12% Bis-Tris, Invitrogen) were loaded with 2 – 14 μ L of lysate per lane (load volumes were adjusted to avoid overloading and smearing, diluting the lysates with additional 1x NuPAGE LDS buffer as necessary). Gel electrophoresis was run for 10 min at 100 V and 15 min at 160 V. Excised gel sections were washed (50% 0.2 M ammonium bicarbonate (AB) solution, 50% acetonitrile (ACN), 30 min at 37 °C), dried by lyophilization, incubated with a reducing agent (20 mM tris(2-carboxyethyl)phosphine (TCEP) in 25 mM AB solution at pH 8.0, 15 min at 37 °C) and alkylated (40 mM

iodoacetamide (IAM) in 25 mM AB solution at pH 8.0, 30 min at 37 °C). The gel sections were dried by lyophilization before in-gel trypsinization (20 µg/mL sequencing grade modified trypsin in buffer as described in the manufacturer's protocol (Promega), 18 hr at 37 °C with gentle shaking). The resulting solutions of tryptic peptides were acidified by addition of 50% digest dilution buffer (60 mM AM solution with 3% formic acid).

Peptide separations (5 µL injection volume) were performed on 15-cm PicoFrit column (75 µm inner diameter, New Objective) packed with Magic 5 µm C18 reversed-phase resin (Michrom Bioresources) using a nanoflow high-pressure liquid chromatography system (Eksigent Technologies), which was coupled online to a hybrid LTQ-Orbitrap XL mass spectrometer (Thermo Fisher Scientific) via a nanoelectrospray ion source. Chromatography was performed with Solvent A (Milli-Q water with 0.1% formic acid) and Solvent B (acetonitrile with 0.1% formic acid). Peptides were eluted at 200 nL/min for 3–28% B over 42 min, 28–50% B over 26 min, 50–80% B over 5 min, 80% B for 4.5 min before returning to 3% B over 0.5 min. To minimize sample carryover, a fast blank gradient was run between each sample. The LTQ-Orbitrap XL was operated in the data-dependent mode to automatically switch between full scan MS ($m/z = 350$ –2000 in the orbitrap analyzer (with resolution of 60,000 at m/z 400) and the fragmentation of the six most intense ions by collision-induced dissociation in the ion trap mass analyzer.

Raw mass spectroscopy data was processed using Elucidator (version 3.3, Rosetta Biosoftware). Peptide and protein annotations were made using SEQUEST (version 28, Thermo Fisher Scientific) with full tryptic digestion and up to 2 missed cleavage sites. Peptide masses were selected between 800 and 4500 amu with peptide mass tolerance of 1.1 amu and fragment ion mass tolerance of 1.0 amu. Peptides were searched against databases compiled from UniRef100 mouse and human, plus contaminants and a reverse decoy database. The peptide database was modified to search for alkylated cysteine residues (monoisotopic mass change, $\Delta = +57.021$ Da) and oxidized methionine ($\Delta = +15.995$ Da). In proteomic profiling experiments, we also considered the acetylation of lysine ($\Delta = +42.011$ Da), methylation of lysine and arginine ($\Delta = +14.016$ Da) and phosphorylation of serine, tyrosine, threonine, histidine and aspartate ($\Delta = +79.966$ Da). Ion currents of modified peptides were summed with their parent peptide. Peptides derived from trypsin or keratin were considered to be contaminants and were not used in subsequent calculations.

Micropipette aspiration. Micropipette aspiration was performed as described previously (Pajerowski *et al.*, 2007), (Swift *et al.*, 2013b). For nucleus aspiration cells were treated with 0.2 $\mu\text{g/ml}$ Latrunculin A (Sigma) for 1 hour at 37°C, detached with trypsin/EDTA, centrifuged and resuspended in aspiration buffer of 135 mM NaCl, 5mM KCl, 5 mM HEPES, 1.8 mM CaCl₂, 2 mM MgCl₂, 2% BSA, 1:3000 propidium iodide (Molecular Probes). Nuclei were stained with Hoechst 33342 (Molecular Probes). Nuclei were aspirated under negative pressure inside a micropipette and the membrane extension was imaged with Nikon TE300 inverted microscope coupled with a digital CCD camera (Roper Scientific, Tuscan AZ), using a 60x oil immersion objective. Suction was applied by syringe and the corresponding pressure was measured by a pressure transducer (Validyne) calibrated by a mercury U-tube manometer. Image analysis was done using ImageJ. The compliance was calculated as described in (Pajerowski *et al.*, 2007) and stiffness is determined from (Majkut *et al.*, 2013). For grafts aspiration a micropipette with diameter of 15 μm is used to deform a freshly excised piece of tissue. After aspiration, the graft was divided in two pieces and one was treated with transglutaminase (Sigma-Aldrich T5398, concentration 100 $\mu\text{g/mL}$ in of 50 mM TRIS buffer, 5 mM CaCl₂, 2 mM dithiothreitol at pH 7.4) for 30 minutes at 37^o C and 5% CO₂ and aspirated again and the other one was treated without transglutaminase and it was used as a control.

MSC xenografts in mouse. All animal experiments were planned and performed according to IACUC protocols. Fresh human bone marrow mesenchymal stem cells were isolated from bone marrow (anonymous donors with Institutional Review Board approvals) from the Xenograft Core Facility at the University of Pennsylvania School of Medicine. MSC were cultured and expanded cultured in low glucose Dulbecco's modification of Eagle's medium (DMEM, Invitrogen) with 10% fetal bovine serum (FBS, Sigma Aldrich) and are used at low passage ($P < 5$). 2×10^6 cells were mixed with Matrigel (#356234, BD Biosciences) according to the manufacturer protocol and injected subcutaneously in mice flank. Cells were either not treated or pretreated with osteogenic media and RA antagonist CD 2665 (1 μM , Tocris Bioscience) for 3 days. Mouse grafts that were isolated after 4weeks growth were also mixed with DiR (Life Technologies) labeled beads prior to injection to insure the proper identification of the human cells localization upon extraction. Grafts that were left to grow for 12 weeks were not mixed with fluorescent

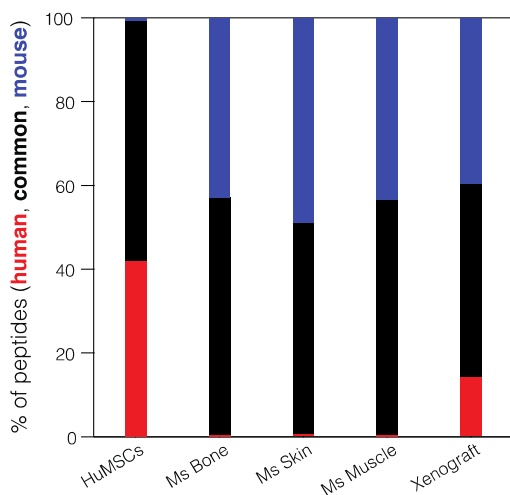
beads, their location was identified by imaging mouse injected with OsteoSense 750EX Fluorescent Imaging Agent (PerkinElmer) 24 hours earlier. After harvesting graft tissues and tissues from skin and bone, each tissue were cut into 3 pieces. One set of tissues were snap-frozen with liquid nitrogen for MS evaluation and the second and third set were fixed with PFA and stained for Alkaline Phosphatase Activity (ALP) and Alizarin red.

ALP and Alizarin Red staining. ALP staining of cells or tissues is performed immediately after their fixation in PFA. After washing with 10mM Tris buffer pH 7.2 samples were immersed in alkaline-dye solution of Fast Blue RR Salt (Sigma FBS-25) capsules dissolved in DW at concentration as it is indicated by the manufacturer and Naphthol AS-MX phosphatase solution. For Alizarin red staining, samples were washed with DW and immersed for 5 to 10 min in 1% Alizarin Red S (LC 106007) pH 4-4.3. After washing with DW the samples are imaged with color camera in bright field. The ALP or Alizarin Red is quantified from the blue or the red component respectively of the color images after deconvolution with Image J. The scale of the single color intensity (0-255) is inverted and normalized by the number of the pixels of the image.

Supplemental Figures

Figure S1.

A Count of peptides that are common or unique to mouse or human in cell, tissue and xenograft samples



B Collagen-I protein and transcript quantified across a range of tissues

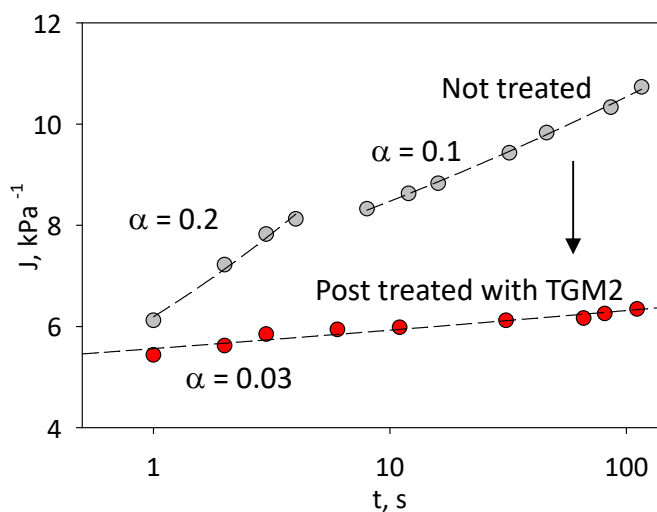
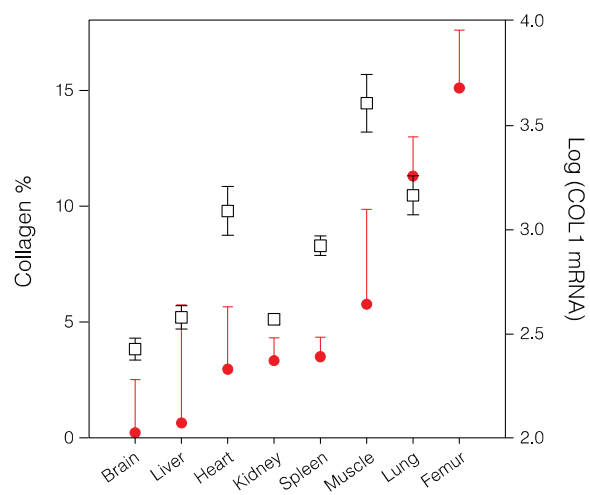
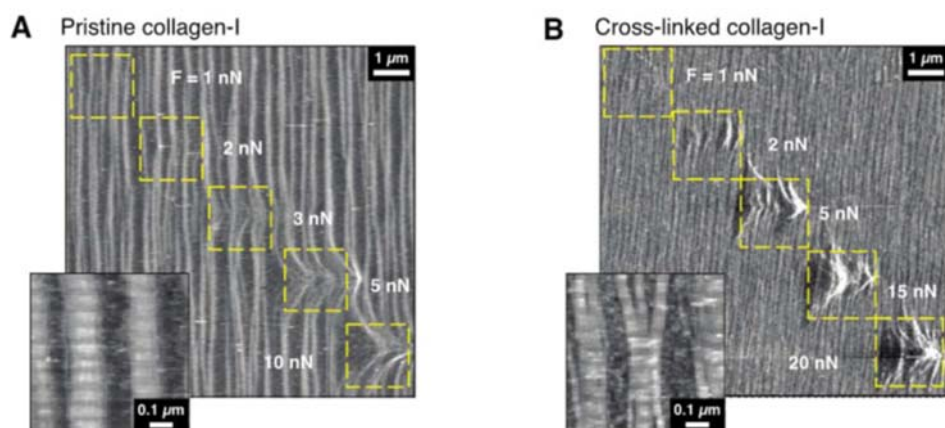


Fig. S1. (A) Human MSCs, primary mouse tissues (bone skin and muscle) and a xenograft (human MSCs in mouse flank, 4 weeks growth) were profiled by mass spectrometry proteomics. By comparison to databases (SEQUEST and NCBI BLAST), peptides were classified as being unique to mouse, human or common to both species. Samples from singular sources had ~ 44% uniquely native peptides and a low

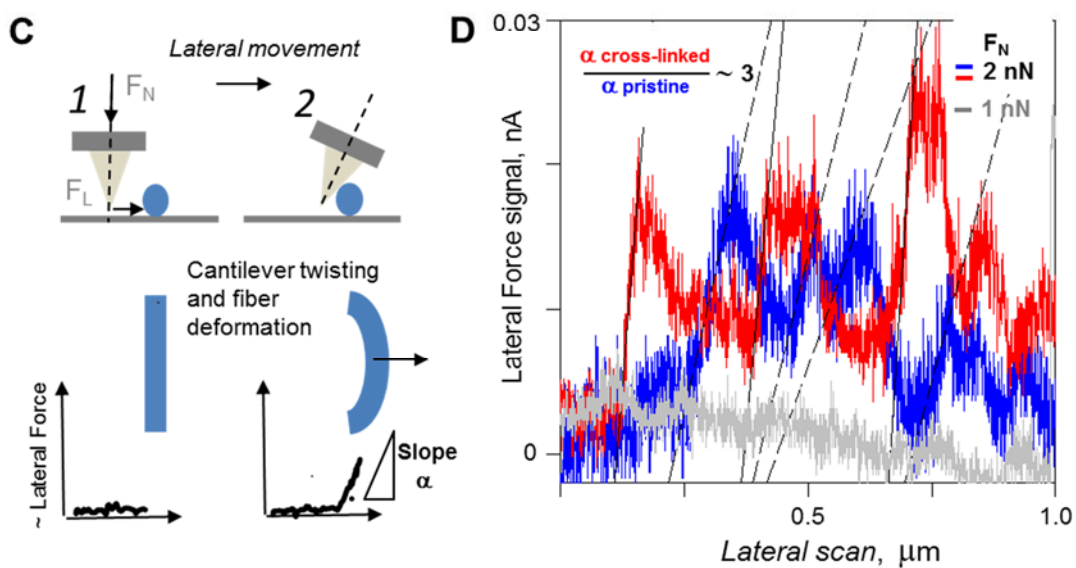
false positive rate of identifying foreign material ($< 0.8\%$ when considering peptides from proteins detected with two-or-more peptides-per-protein). The xenograft sample contained a significant number of human peptides, confirming that material derived from the MSCs persisted in the tumor for at least 4 weeks. A protein level analysis of the samples is shown in Fig. 2A. (B) Earlier work has shown that collagen protein and transcript levels are higher in stiffer tissues (Neuman and Logan, 1950). (C) Compliance of the excised xenograft aspirated for 100 sec is calculated as described in with α being higher for more viscous materials (Pajeroski *et al.*, 2007). The power law fit shows that a 30 min treatment with transglutaminase (TGM2) makes the tissue less viscous and less compliant, consistent with being more solid-like and stiffer.

Figure S2.

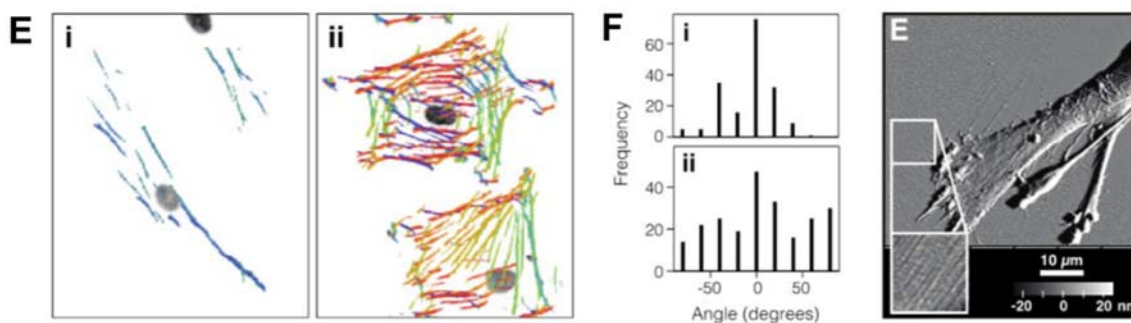
AFM scratching with increasing normal force shows robustness of cross-linked collagen-I film

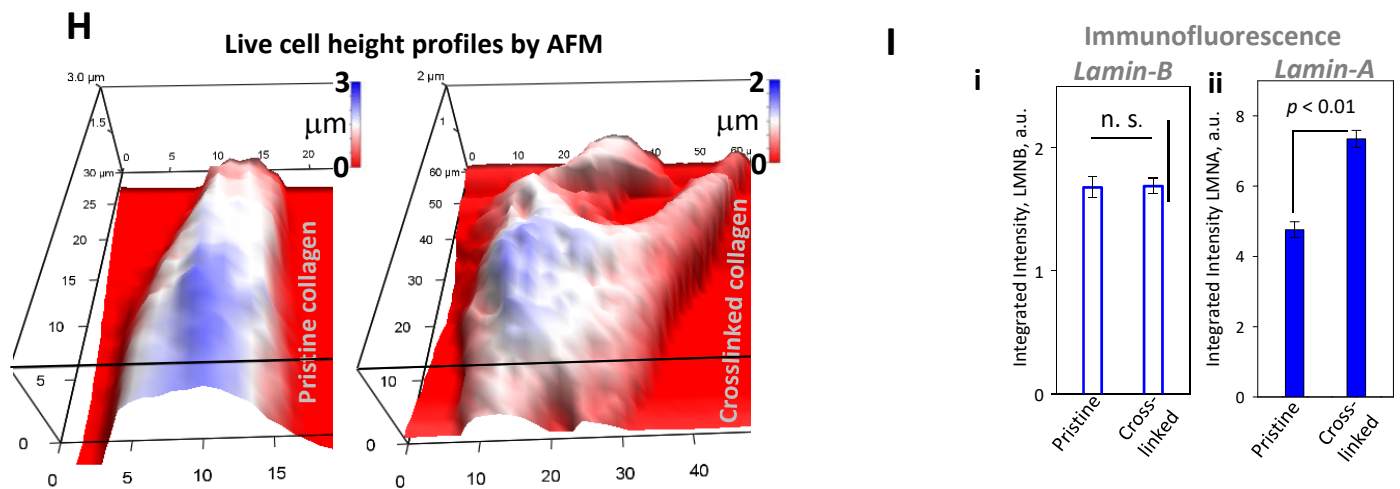


Fibril resistance to lateral forces torques the AFM tip



Orientation of stress fibers on pristine and cross-linked collagen-1 films





S2. Scratching the surface of (A) pristine and (B) cross-linked collagen-I films with the tip of an AFM demonstrates the increased robustness of the cross-linked film. Insets show high-resolution images of collagen fibrils. (C) Schematic representation of the lateral movement of the AFM tip and interaction with a fibril. (D) Lateral Force signal (not calibrated) versus scan distance for pristine and crosslinked collagen films. In gray is shown the signal for 1nN loading force. When the tip is dragged across the fibrils with 2 nN loading force the tip is tilted due to the resistance felt by the collagen fibril and the fibrils are deformed to a point after which the tip slips over the fibril. Force – distance slopes on the fibrils on crosslinked films are consistently higher than those of pristine films with ratio between the averaged slopes ~ 3 . (E) Orientation of stress fibers in cells on (i) pristine collagen-1 and (ii) cross-linked films determined by a segmentation algorithm with different colors representing different directions of the fibers (Zemel *et al.*, 2010). Stress fibers are tightly aligned with the collagen fibrils on pristine films, but are at broadly distributed orientations on the cross-linked films. (F) Angle distributions of stress fibers in MSCs cultured on (i) pristine or (ii) cross-linked collagen-I films, with angles measured with respect to the long axis of the ellipse fitted to each individual cell. (G) AFM topography image of an MSC cultured for 5 days on a cross-linked collagen-1 film. Inset highlights the fibrillar collagen. (H) AFM images made in Force Volume mode of life cells on pristine and cross-linked films. (I) Cells spread on gels with different stiffness for 24 h hours and co-stained for Lamin-A and Lamin-B, have constant total lamin-B whereas lamin-A is increased with $\sim 50\%$

Figure S3.

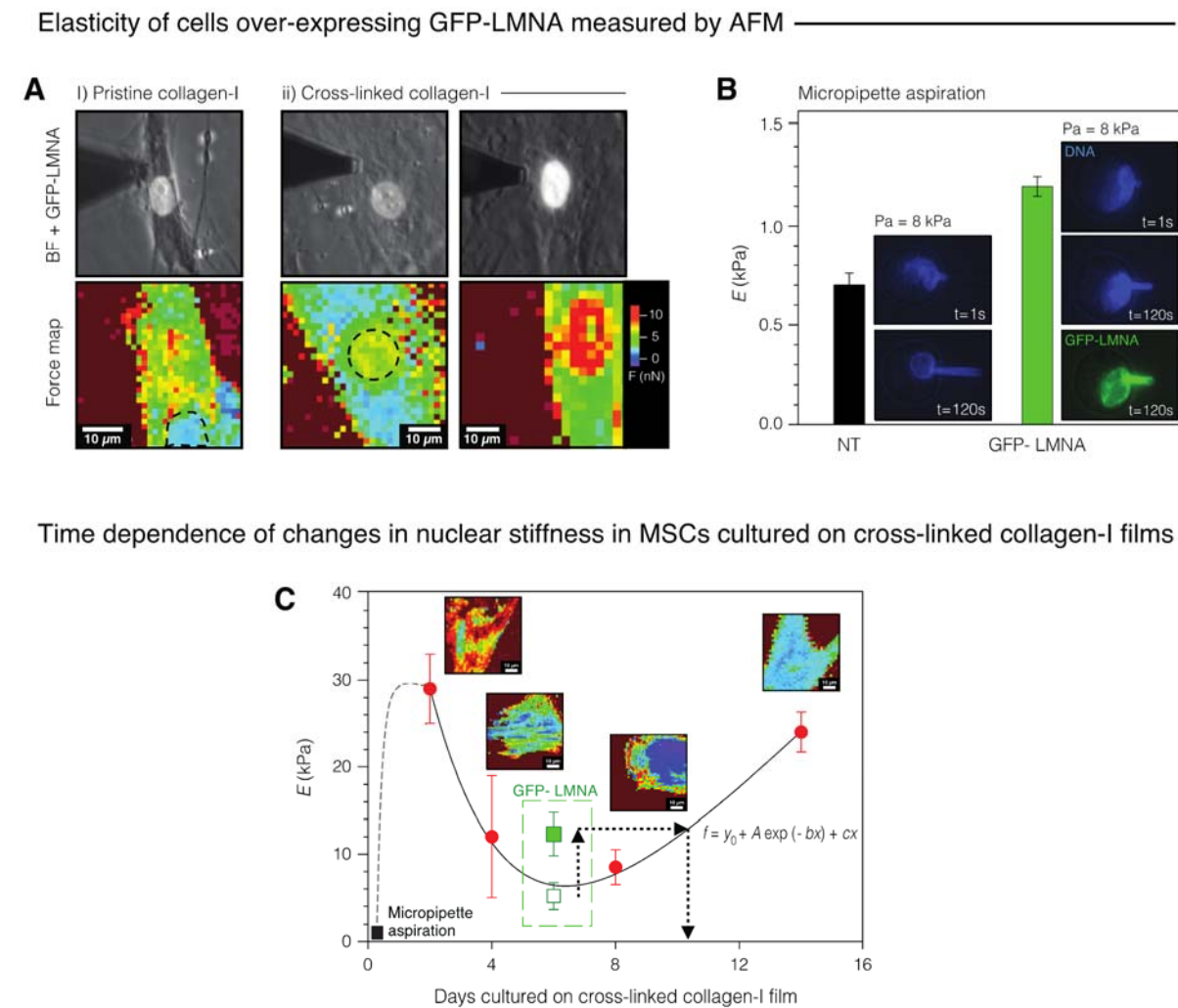


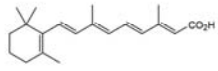
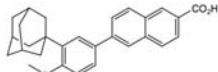
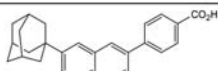
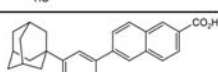
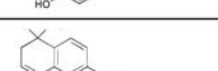
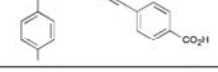
Fig. S3. (A) Phase contrast images (upper row) and their corresponding AFM elasticity maps of GFP-lamin-A transduced MSCs cultured for 6 days on (i) pristine and (ii) cross-linked thin collagen films show correlation of lamin-A expression and the stiffness of the nucleus. (B) Young's moduli of nuclei of native and lamin-A overexpressing MSC cells measured with micropipette aspiration after treatment with latrunculin. Insets – images of nuclear deformation for different time points: blue = Hoechst; green = GFP-lamin-A. (C) Time-resolved progression of cell elasticity at nuclear positions for MSCs cultured on cross-linked film. Although the extracellular environment is subjected to constant remodeling by cells *in vivo*, the

matrix is actually a comparatively passive mechanical stimuli that changes slowly compared to the dynamic remodeling of cellular actomyosin. To better understand the dynamic internal adaptation in response to changes in substrate mechanics, we measured changes in the elastic response of the nuclear region, as measured by AFM, in MSCs on cross-linked collagen films over a period of 2 weeks. Elasticity maps of cells cultured on films for 48 hours gave a mean E of about 30 kPa and revealed a highly heterogeneous response within cells. After 2 more days in culture, the elasticity of the nuclear region dropped to 10 kPa, suggesting that cells undergo a relaxation of cortical tension after an initial stage of intensive cytoskeletal remodeling. The stiffness continued to decrease monotonically for a week following plating before rising again after two weeks, with a far more homogeneous response over the entire cell. The elastic response at this late culture point became more complicated due to the establishment of cell-cell contacts and cell-induced matrix remodeling. However, up to 1 week following initial plating, we were able to make measurements only on isolated cells and topographical AFM images revealed no deposition of matrix. Plot shows mean values of Young's moduli obtained from the elasticity maps at the nuclear region and averaged from ~ 60 curves per cell and from 4 - 7 individual cells per day.

Figure S4.

Agonists and antagonists to the RA pathway

A

Compound	Description	Structure	Kd (nM)			Reference
			RAR α	RAR β	RAR γ	
All-trans retinoic acid ("RA")	Pan-RAR agonist		16 15 16 14	5 13 7 11	3 18 3 16	(Bernard, 1992) (Agarwal, 1996) (Szondy, 1997) (Gambone, 2002)
Adapalene	RAR β , γ agonist		1100	34	130	(Shroet, 1997)
CD1530	RAR γ agonist		2750	1500	150	(Bernard, 1992)
CD437	RAR γ agonist		6500	2480	77	(Bernard, 1992)
AGN193109 ("AGN")	Pan-RAR antagonist		22	8	7	(Gambone, 2002)
CD2665	RAR γ antagonist		> 1000	306	110	(Szondy, 1997)

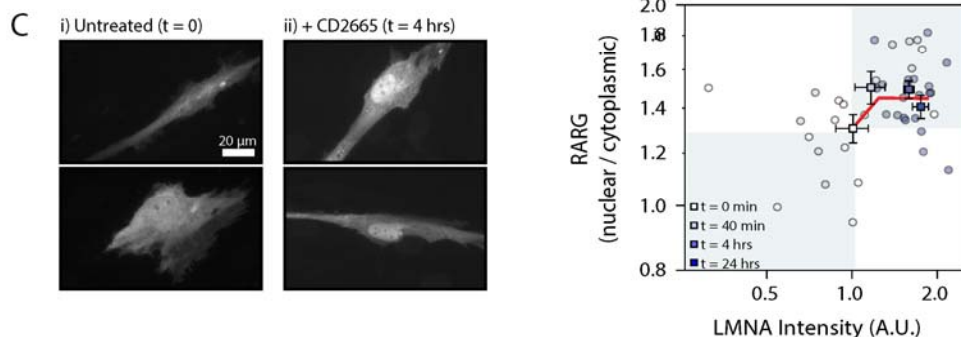
Response in LMNA levels to RA pathway perturbations in MSCs

B

Sample identity	Passage number	Substrate	Time in culture	Method	Agonist	Antagonist	LMNA (Antagonist/Agonist)
MSC, 46 y.o. male	4	40 kPa gel	4 days	IF	RA	AGN	1.14
MSC, #1	3	glass	3 days	IF	CD1530	CD2665	1.17
MSC, 46 y.o. male	4	plastic	4 days	IF	RA	AGN	1.19
MSC, #1	3	cross-linked film	3 days	IF	CD1530	CD2665	1.39
MSC, 23 y.o. male	6	plastic	4 days	IF	CD1530	CD2665	1.39
MSC, 49 y.o. male	4	plastic	4 days	IF	RA	AGN	1.41
MSC, 30 y.o. female	6	plastic	6 days	Wb	RA	AGN	1.49
MSC, 30 y.o. female	6	plastic	8 days	MS	RA	AGN	1.71
MSC, 23 y.o. male	6	plastic	4 days	IF	RA	AGN	1.96
MSC, 23 y.o. male	5	plastic	4 days	IF	RA	AGN	2.04
MSC, 43 y.o. male; 46 y.o. female	5	plastic	36 hrs	Wb	RA	AGN	2.37
MSC, 43 y.o. male; 46 y.o. female	5	40 kPa gel	36 hrs	Wb	RA	AGN	2.76
MSC, 30 y.o. female	6	plastic	8 days	Wb	RA	AGN	3.63

AVG \pm SEM, 1.8 \pm 0.2

RARG construct's rapid kinetics with antagonist stimulation consistent with rapid increase in LMNA

Fig. S4. (A) Table of properties of drugs that affect the RA pathway (Bernard *et al.*, 1992);(Agarwal *et al.*,

1996);(Szondy *et al.*, 1997);(Shroot and Michel, 1997);(Gambone *et al.*, 2002). (B) Table of MSC responses to agonists and antagonists to the RA pathway while cultured on stiff substrates, quantified by immunofluorescence (IF), western blot (Wb) and mass spectrometry (MS). The last column is averaged for each donor in Fig. 5B. (C) MSCs expressing the fluorescent RARG construct 'GEPRA' ("genetically encoded probe for RA" (Shimozono *et al.*, 2013)) cultured on plastic in the (i) absence and (ii) with the addition of RARG antagonist CD2665 for four hours. (iii) LMNA level, as determined by immunofluorescence, responded rapidly to the addition of CD2665, showing a 50% increase with an exponential half-life of ~ 2 hours. Consistent with Fig. 4Fiii, this process was concomitant with an increase in nuclear localization of transcription factor RARG.

Figure S5.

Response of LMNA levels to RA pathway perturbations in MSCs derived from iPS cells.

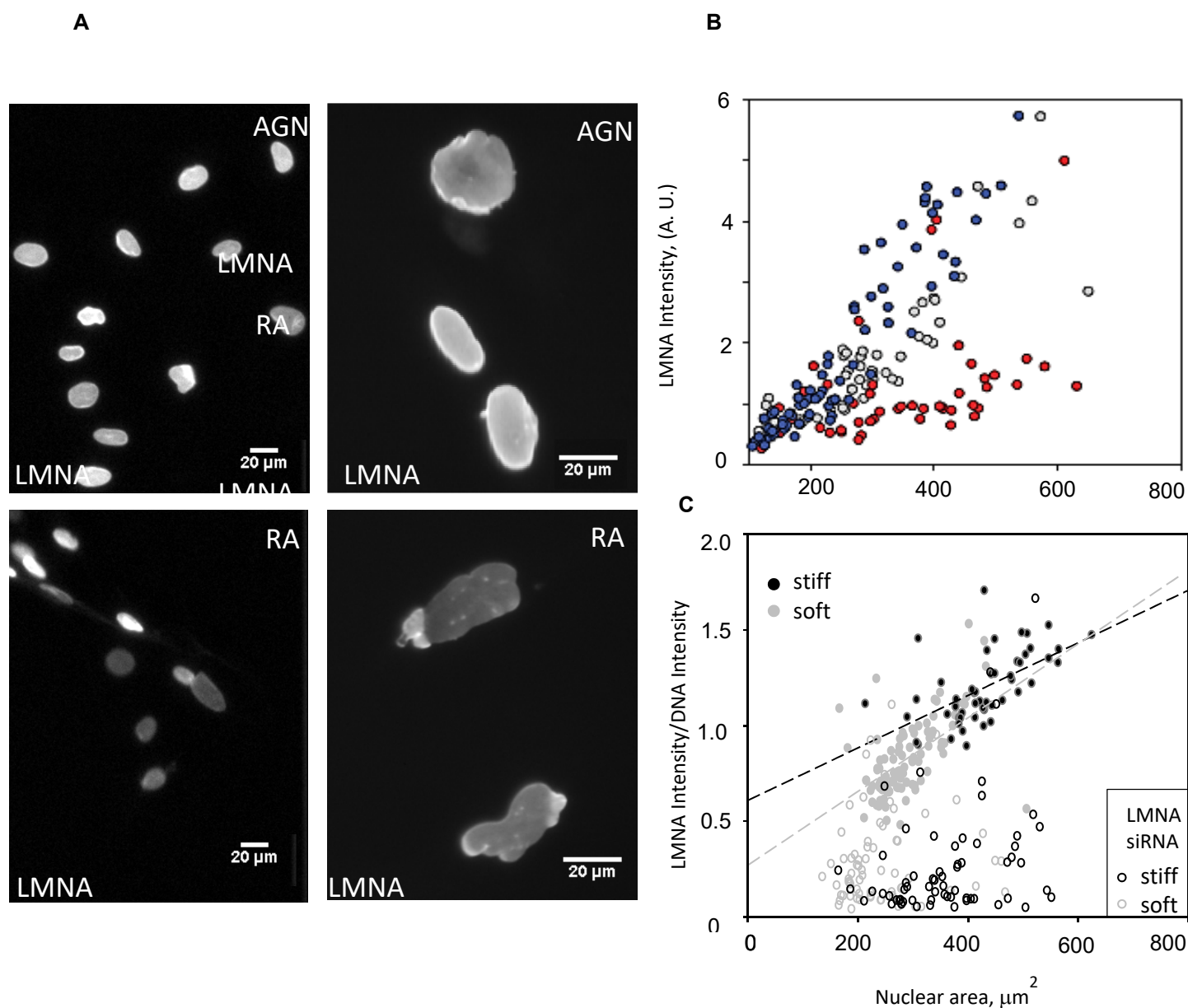
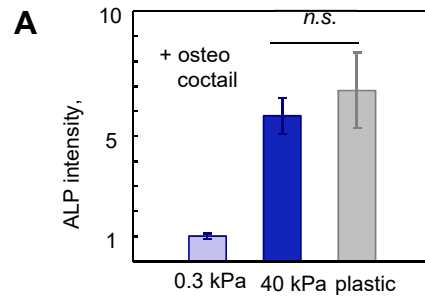


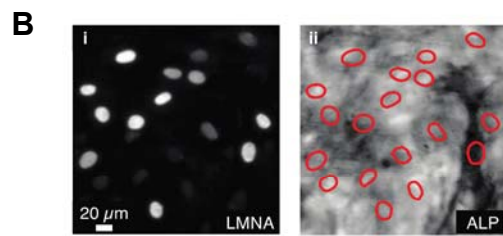
Fig. S5. (A) iPS cells differentiated to MSCs express LMNA as shown by immunofluorescent imaging, and the cells respond to AGN (upper images) and RA (lower images) treated for 4 days on plastic. (B) The corresponding LMNA quantification as determined by immunofluorescence, empty symbols – control, blue AGN, red RA. (C) IF of LMNA integrated intensity normalized with DNA integrated intensity (labeled with Hoescht) as a function of the nuclear area shows that data on soft and stiff substrate have similar slope and LMNA knockdown eliminates the nuclear spread area dependence.

Figure S6

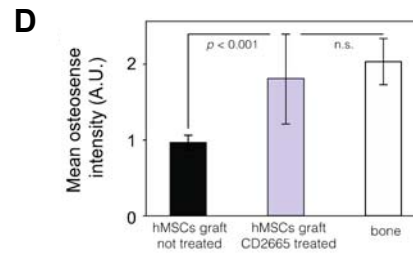
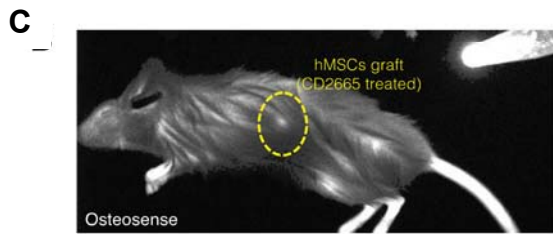
ALP staining in MSCs on gels and plastic *in vitro*



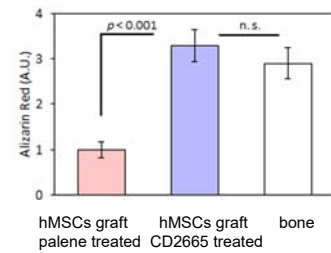
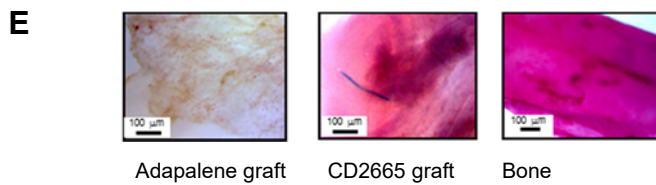
Cell-by-cell measurement of ALP staining in MSCs treated with RA antagonist *in vitro*



Osteosense imaging in live mice shows greater osteogenesis in xenograft tumors pretreated with RARG specific antagonist



Alizarin Red staining of Agonist (CD26650) and Antagonist (Adapalene) pretreated grafts



Antagonist increases *in vivo* osteogenesis: ALP staining

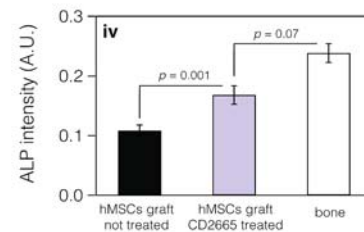
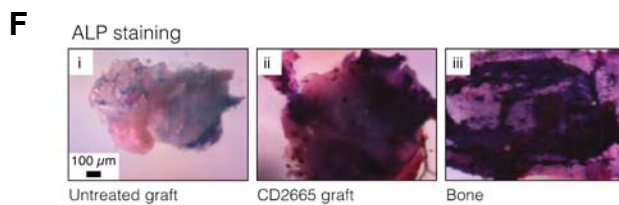


Fig. S6. (A) MSCs cultured on 40 kPa gel and plastic (rigid $E \sim$ GPa) in presence of osteo cocktail, show no significant difference in their osteogenic activity evaluated by the ALP signal and normalized to MSCs ALP signal on soft gel. (B) MSCs on rigid substrate were treated with a combination of osteo-induction media (OIM) and RARG-specific antagonist CD2665 (Fig. 5F). Osteogenic potential was estimated on a cell-by-cell basis and correlated with individual cellular levels of LMNA (i), by identifying and integrating ALP staining within the area of the nucleus (ii). (C) Further analysis of hMSCs grafted into mouse flank following pre-treatment with an RARG-specific antagonist is consistent with increased osteogenesis (see also Fig. 5G). Live mouse imaged after 12 weeks of MSCs graft growth with osteosense contrast agent (control tube in top right of image) used to show the location of a subcutaneous graft pre-treated with RA-pathway antagonist CD2665. (D) Quantification of osteosense intensity suggests a significant increase in osteogenic character in grafts from MSCs pre-treated with CD2665. Error bars show standard deviation. (E) Alizarin red staining of hMSCs subcutaneous grafts pretreated with RARG-specific agonists Adapalene and antagonist CD2665 compared to bone shows that the antagonist enhanced osteogenesis and agonist suppressed osteogenesis *in vivo*. (F) In separate experiment excised tissues of MSCs antagonist pretreated graft was stained with ALP and compared to bone and untreated graft: (i) graft from untreated MSCs; (ii) graft from MSCs pre-treated for three days with CD2665; (iii) mouse bone, (iv) Quantification of ALP intensity.

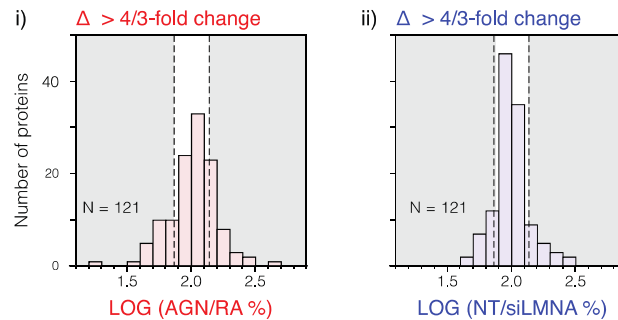
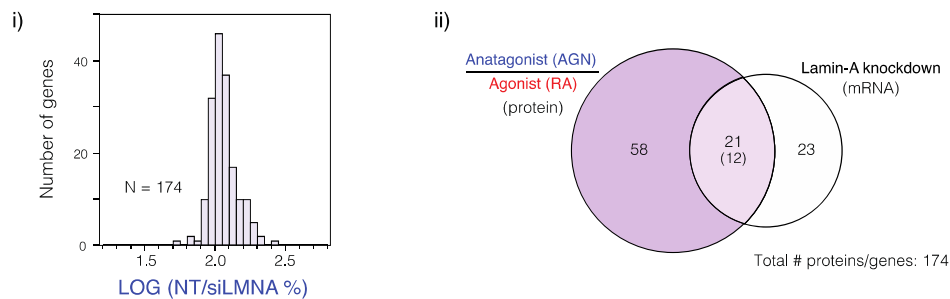
Figure S7.**A** Changes to the proteome induced by perturbation to the RA-pathway or siLMNA**B** Comparison of proteome changes during RA-treatment and mRNA changes with siLMNA

Fig. S7. Proteomic profiling of MSCs subjected to lamin knockdown or perturbation to the retinoic acid (RA) pathway. (A) Histograms showing the width of distribution of protein level changes induced in MSCs by (i) RA-pathway antagonist AGN vs. agonist RA (ii) untreated vs. siLMNA. The levels of 121 proteins common to both samples were quantified by mass spectrometry (MS) with a minimum of 3 tryptic peptides detected per protein (see Figs. 6A, B). (B) Protein changes during RA-pathway perturbation were also compared to transcript changes during LMNA knockdown. (i) Histogram showing changes in levels of 174 mRNA transcripts, quantified by microarray, that were also quantified by MS. (ii) Venn diagram showing the proteins and transcripts that varied by more than 4/3-fold. 21 genes/proteins changed in both experiments, and of these, 12 showed correlated changes. The genes/proteins common to this overlap set and that shown in Fig. 6B are: ALCAM, STAT1, LMNA, EHD2, MVP and P4HA2.

Supplemental references

Agarwal, C., Chandraratna, R.A.S., Johnson, A.T., Rorke, E.A., and Eckert, R.L. (1996). AGN193109 is a highly effective antagonist of retinoid action in human ectocervical epithelial cells. *Journal of Biological Chemistry* **271**, 12209-12212.

Bernard, B.A., Bernardon, J.M., Delescluse, C., Martin, B., Lenoir, M.C., Maignan, J., Charpentier, B., Pilgrim, W.R., Reichert, U., and Shroot, B. (1992). Identification of synthetic retinoids with selectivity for human nuclear retinoic acid receptor-gamma. *Biochemical and Biophysical Research Communications* **186**, 977-983.

Buxboim, A., Rajagopal, K., Brown, A.E.X., and Discher, D.E. (2010). How deeply cells feel: methods for thin gels. *Journal of Physics-Condensed Matter* **22**.

Gambone, C.J., Hutcheson, J.M., Gabriel, J.L., Beard, R.L., Chandraratna, R.A.S., Soprano, K.J., and Soprano, D.R. (2002). Unique property of some synthetic retinoids: Activation of the aryl hydrocarbon receptor pathway. *Molecular Pharmacology* **61**, 334-342.

Majkut, S., Idema, T., Swift, J., Krieger, C., Liu, A., and Discher, D.E. (2013). Heart-Specific Stiffening in Early Embryos Parallels Matrix and Myosin Expression to Optimize Beating. *Current Biology* **23**, 2434-2439.

Neuman, R.E., and Logan, M.A. (1950). The determination of collagen and elastin in tissues. *Journal of Biological Chemistry* **186**, 549-556.

Pajerowski, J.D., Dahl, K.N., Zhong, F.L., Sammak, P.J., and Discher, D.E. (2007). Physical plasticity of the nucleus in stem cell differentiation. *Proceedings of the National Academy of Sciences of the United States of America* **104**, 15619-15624.

Shimozono, S., Imura, T., Kitaguchi, T., Higashijima, S., and Miyawaki, A. (2013). Visualization of an endogenous retinoic acid gradient across embryonic development. *Nature* **496**, 363-366.

Shroot, B., and Michel, S. (1997). Pharmacology and chemistry of adapalene. *Journal of the American Academy of Dermatology* **36**, 96-103.

Swift, J., Harada, T., Buxboim, A., Shin, J.-W., Tang, H.-Y., Speicher, D.W., and Discher, D.E. (2013a). Label-free mass spectrometry exploits dozens of detected peptides to quantify lamins in wildtype and knockdown cells. *Nucleus-Austin* **4**, 450-459.

Swift, J., Ivanovska, I.L., Buxboim, A., Harada, T., Dingal, P.C.D.P., Pinter, J., Pajeroski, J.D., Spinler, K.R., Shin, J.-W., Tewari, M., Rehfeldt, F., Speicher, D.W., and Discher, D.E. (2013b). Nuclear lamin-A scales with tissue stiffness and enhances matrix-directed differentiation. *Science* 341, 1240104.

Szondy, Z., Reichert, U., Bernardon, J.M., Michel, S., Toth, R., Ancian, P., Ajzner, E., and Fesus, L. (1997). Induction of apoptosis by retinoids and retinoic acid receptor gamma-selective compounds in mouse thymocytes through a novel apoptosis pathway. *Molecular Pharmacology* 51, 972-982.

Zemel, A., Rehfeldt, F., Brown, A.E.X., Discher, D.E., and Safran, S.A. (2010). Optimal matrix rigidity for stress-fibre polarization in stem cells. *Nature Physics* 6, 468-473.

Zou, L.J., Luo, Y.L., Chen, M.W., Wang, G., Ding, M., Petersen, C.C., Kang, R., Dagnaes-Hansen, F., Zeng, Y.L., Lv, N.H., Ma, Q., Le, D.Q.S., Besenbacher, F., Bolund, L., Jensen, T.G., Kjems, J., Pu, W.T., and Bunger, C. (2013). A simple method for deriving functional MSCs and applied for osteogenesis in 3D scaffolds. *Scientific Reports* 3.